

Supplementary material

Multi-scale modeling method

To address the failure mechanism of the intermediate filament meshwork, the interpretation of the dynamic fracture property of the intermediate filament meshwork requires a large scale meshwork model (in the order of μm^1) as well as accurate representation of the dynamical property of each filament and their interactions with atomic interaction detail (in the order of \AA^2). Thereby, the multi-scale modeling can be a strategy combining accuracy and efficiency³, which includes the full atomic modeling for single filaments and the mesoscopic model for intermediate filament meshwork. The full atomic model provides an accurate description of the physical mechanisms governing the yielding (unfolding of alpha-helics) and stiffening (structural transition) process of each filament under loading, and records the accurate description of the force-extension relation of the single filament during the loading history^{4,5}. The mesoscopic model inherits the physical properties of the former and provides a faithful estimation of dynamic fracture property in the large scale.

Similar model has been used in earlier studies of fracture mechanism in crystalline materials and provides an effective way to describe the nonlinear constitutive behavior based on computationally effective pair potential functions. It is noted that this model does not include the nonbonded interaction because the intermediate filament studied here is fully polymerized with a uniform diameter of 10 nm, which is true for most of intermediate filaments. Therefore the intermolecular interaction is much weaker than its tensile or bending resistance.

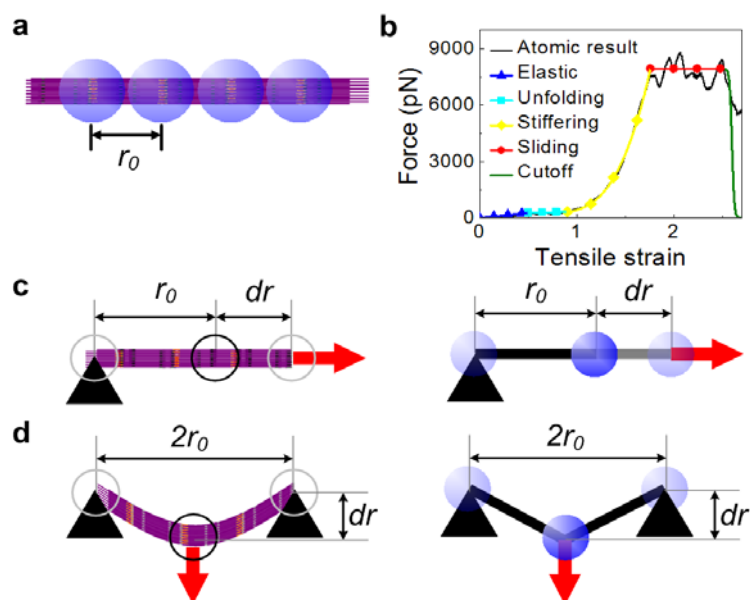


Figure S1. Mechanical loading conditions used to fit tensile (panel c) and bending (panel d) potential parameters for intermediate filament mesoscopic model (panel a). Tensile parameters are fitted so that the force-strain curve of a stretching mesoscopic simulation is identical to the one obtained from an atomistic stretching simulation (panel b). The bending parameters are obtained by identifying the bending stiffness of a three-bead mesoscale model to the bending stiffness of an intermediate filament of the same length by a three-point bending experiment for the same small deformation (panel d).

In Eq. (5), k_i and r_i are spring constants that derived directly from the force-extension curve of the tension test of full atomic model (as shown in Fig. S1b), without empirical fitting. r_0 is the equilibrium distance between pair beads as show in Fig. S1a. Alpha-helix domains within the filament are intact before the extension reaches $r_1 - r_0$ and the slope of the force-extension curve is constant as k_1 . The extension beyond $r_1 - r_0$ leads to the unfolding of the alpha-helix domains until they become nearly fully unfolded at $r_2 - r_0$, and in this extension region the force-extension curve is linear with a slope of k_2 . The third broad region before the extension of $r_3 - r_0$ corresponds to the stiffening of the material because of the alpha-beta transition, and the nonlinearity of the force extension curve is expressed by the polynomial function with stiffness parameters k_3^1 , k_3^2 and k_3^3 . For the forth region, the subunits within the filament slide against each other under a constant force. The parameters R_1 , R_2 and R_3 are calculated from force continuity conditions. The values of these parameters are given in Table 1.

Table 1. Geometric and mechanical parameters for the model.

Parameter and units	Numerical value
Equilibrium bead distance r_0 (in Å)	50
Critical distances r_1, r_2, r_3 (in Å)	75, 95, 138, 180
Tensile stiffness parameters k_1, k_2 (in kcal/mol/Å ²)	0.1595, 0.0324,
Tensile stiffness parameters for the nonlinear region k_3^1 (in kcal/mol/Å ²), k_3^2 (in kcal/mol/Å ³), k_3^3 (in kcal/mol/Å ⁴)	0.2044, 0.0146, 9.2465×10^{-4}
Force continuity conditions R_1, R_2 and R_3 (in kcal/mol/Å)	3.9877, 4.6357, 113.9364
Bond breaking distance r_b (in Å)	180
Equilibrium angle θ_0 (in rad)	π
Bending stiffness parameter k_B (in kcal/mol/rad ²)	169.51
Mass of each mesoscale particle (in amu)	230913
Switch function Ξ	300

Computing Techniques and visualization method

The molecular simulations described here were carried out with the classical MD approach by an extended version of the LAMMPS code⁶. Visualization of atomic and mesoscopic models is done with visual molecular dynamics (VMD) software (hydrogen bonds are defined to be within 5 Å for visualization purposes for atomic models)⁷.

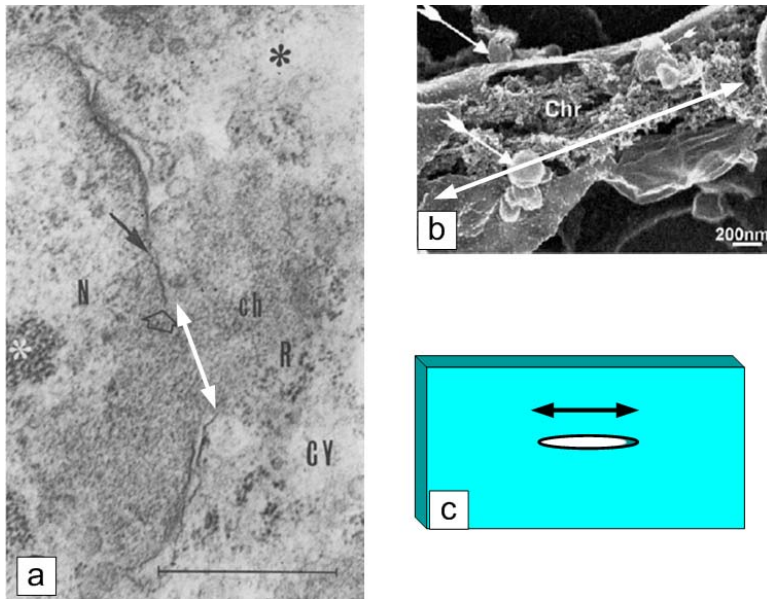


Figure S2. The experimental observations of nuclear envelope rupture. Panel a, adopted from⁸. The Kirkman-Robbin tumour cell after being treated by x-ray irradiation. The black peripheral is the nuclear envelope and the white double arrow indicates the crack. The chromatin (ch) comes from the nucleus (N) through the crack into the cytoplasm (CY) and intermingles with the polyribosomes (R). Scale bar: 500 nm. Panel b, adopted from⁹. Crack forms and propagates during the disassembling process of the nuclear envelope of *Xenopus* egg cell. The chromatin (chr) exposes during such a process and the white double arrow indicates the crack. Scale bar: 200 nm. Panel c, the sketch map of the model used in our study and the black double arrow indicates the crack.

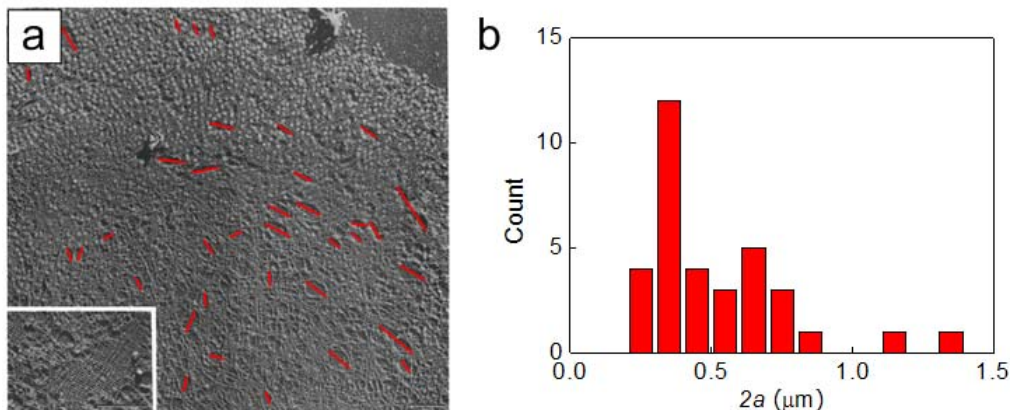


Figure S3. The experimental image of nuclear lamina of *Xenopus* oocytes and the distribution of imperfections on the network material. Panel a, adopted from¹. Freeze-dried/metal-shadowed nuclear envelope, revealing the structure of nuclear lamina meshwork partially covered with arrays of nuclear pore complexes (bars, 1 μm). Imperfections on the meshwork are highlighted by red bars for their long axis. Panel b, The histogram of lengths of the imperfections as shown in panel a.

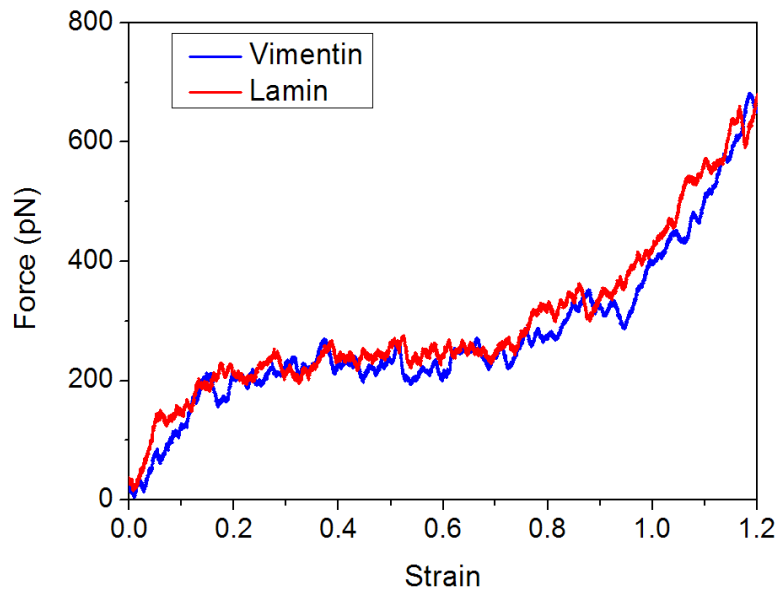


Figure S4. The force-extension curve of atomistic model of a lamin dimer and a vimentin dimer (at a loading rate of 0.01 Å/ps and probed by steered molecular dynamics). The overall agreement of the two curves are caused by the fact that the overall structure of the rod-like domain of vimentin and lamin are both composed of coiled-coil structures.

Supplementary references

1. Aebi, U.; Cohn, J.; Buhle, L.; Gerace, L., The Nuclear Lamina Is a Meshwork of Intermediate-Type Filaments. *Nature* **1986**, 323 (6088), 560-564.
2. Ackbarow, T.; Chen, X.; Keten, S.; Buehler, M. J., Hierarchies, multiple energy barriers, and robustness govern the fracture mechanics of alpha-helical and beta-sheet protein domains. *Proceedings of the National Academy of Sciences of the United States of America* **2007**, 104 (42), 16410-16415.
3. Buehler, M. J., Nature designs tough collagen: Explaining the nanostructure of collagen fibrils. *Proceedings of the National Academy of Sciences of the United States of America* **2006**, 103 (33), 12285-12290.
4. Qin, Z.; Buehler, M. J., Molecular dynamics simulation of the alpha-helix to beta-sheet transition in coiled protein filaments: evidence for a critical filament length scale. *Phys Rev Lett* **2010**, 104 (19), 198304.
5. Qin, Z.; Kreplak, L.; Buehler, M. J., Hierarchical structure controls nanomechanical properties of vimentin intermediate filaments. *PLoS ONE* **2009**, 4 (10), e7294.
6. Plimpton, S., Fast Parallel Algorithms for Short-Range Molecular-Dynamics. *Journal of Computational Physics* **1995**, 117 (1), 1-19.
7. Humphrey, W.; Dalke, A.; Schulten, K., VMD: visual molecular dynamics. *J Mol Graph* **1996**, 14 (1), 33-8, 27-8.
8. Djaczenk, W.; Starzyk, H.; Rzucidlo, Z., X-Ray-Irradiation Induced Changes of Nuclear Membrane of Kirkman-Robbins Tumor-Cells. *Experientia* **1973**, 29 (1), 83-84.
9. Cotter, L.; Allen, T. D.; Kiseleva, E.; Goldberg, M. W., Nuclear membrane disassembly and rupture. *J Mol Biol* **2007**, 369 (3), 683-95.